

# Hybrid Dual-Loop Control of PV DC-DC Boost Converters Using Type-2 Fuzzy Logic and Model Predictive Control

Nesrine Cherigui<sup>1,2</sup>, Abdelkarim Chemidi<sup>1,3,\*</sup>, Ahmed Tahour<sup>1</sup>

<sup>1</sup>*Ecole Supérieure en Sciences Appliquées Tlemcen,  
BP 165 RP Bel Horizon, 13000 Tlemcen, Algeria*

<sup>2</sup>*Laboratoire d'Automatique Tlemcen,  
Chetouane, BP 230, 13000 Tlemcen*

<sup>3</sup>*Manufacturing Engineering Laboratory of Tlemcen,  
Chetouane, BP 230, 13000 Tlemcen*

*Nesrine.cherigui@essa-tlemcen.dz; \*abdelkarim.chemidi@univ-tlemcen.dz; ahmed.tahour@essa-tlemcen.dz*

**Abstract**—This paper presents a hybrid dual-loop control strategy for a standalone photovoltaic energy system interfaced with a boost converter. Photovoltaic systems exhibit strong non-linear behavior and high sensitivity to irradiance, temperature, and load variations, which makes voltage regulation and dynamic performance challenging, in especially with a single-loop control configuration. To address these issues, a cascaded control architecture is proposed, where an outer voltage regulation loop based on Type-2 fuzzy logic generates a robust reference current, while an inner loop based on model predictive control ensures fast and accurate inductor current tracking. A comparative study with a Type-1 fuzzy logic-based predictive control strategy is conducted using dynamic performance indicators. Simulation results show that both strategies achieve overshoot free voltage regulation, while the proposed Type-2 fuzzy logic-based approach reduces the response and settling times by approximately twenty-one percent. In addition, the proposed fuzzy logic and predictive control architecture demonstrate a strong disturbance rejection capability under varying environmental and load conditions, confirming its effectiveness for high performance photovoltaic power conversion applications.

**Index Terms**—DC-DC power converters; Photovoltaic systems; Predictive control; Type-2 fuzzy logic control.

## I. INTRODUCTION

The continuous advancement in science and technology has led to a steady increase in global electrical energy demand [1]. In this context, the transition to renewable energy sources has become a critical priority to address environmental concerns and the limited availability of fossil fuels. Among renewable technologies, photovoltaic (PV) systems have gained significant attention due to their modularity, environmental friendliness, low maintenance requirements, and silent operation [2]. However, the electrical power extracted from PV systems is strongly influenced by environmental conditions, particularly solar irradiance and ambient temperature variations [3], which directly affect the system efficiency and stability.

To ensure optimal energy harvesting, PV systems are commonly operated under maximum power point tracking (MPPT) strategies, which aim to maintain the PV array at its optimal operating point under varying conditions [4]. In practical implementations, PV arrays are interfaced with DC-DC power converters to regulate voltage and efficiently transfer power to the load or DC bus. Among various converter topologies, the DC-DC boost converter is widely adopted because of its simple structure, low cost, and ability to increase relatively low PV voltage. Nevertheless, the boost converter exhibits non-minimum phase behavior and unstable zero dynamics, which complicate voltage regulation, especially under fast irradiance variations and load disturbances.

Conventional linear controllers, such as proportional-integral (PI) and proportional-integral-derivative (PID) regulators, are still widely used in industrial PV applications due to their simplicity and ease of implementation [5]. However, their performance is highly dependent on accurate system modeling and fixed-gain tuning, which limits robustness in the presence of non-linearities, parameter uncertainties, and rapidly changing operating conditions. As a result, linear control schemes often lead to excessive overshoot, long settling times, and steady-state oscillations when applied to PV boost converters operating in dynamic environments.

To address these limitations, various non-linear and intelligent control strategies have been investigated. Sliding mode control (SMC) provides strong robustness against disturbances and modeling uncertainties, but often suffers from chattering phenomena and increased switching losses [6]. Intelligent approaches, including fuzzy logic control (FLC) [7], artificial neural networks (ANN) [8], and adaptive neuro-fuzzy inference systems (ANFIS) [9], have demonstrated improved adaptability and robustness without requiring an exact mathematical model. In particular, Type-1 fuzzy logic controllers have shown superior performance compared to classical linear controllers; however, their effectiveness may degrade under significant uncertainty,

measurement noise, and rapid parameter variations [10].

Type-2 fuzzy logic controllers extend the conventional Type-1 fuzzy framework by explicitly incorporating uncertainty into membership functions through the footprint of uncertainty concept, enabling enhanced handling of imprecise information and modeling errors [11]. Despite these advantages, most of the Type-2 fuzzy logic applications reported in PV systems are based on single-loop control structures [12], and their integration within cascaded or dual-loop architectures has not yet been comprehensively explored or quantitatively evaluated.

In parallel, model predictive control (MPC) has emerged as an effective control strategy for power electronic converters due to its fast transient response, ability to explicitly handle constraints, and predictive optimization capability. MPC has been successfully applied to current control of DC-DC converters, achieving accurate tracking and improved dynamic performance [13]. Nevertheless, when employed as a standalone control technique, MPC may exhibit sensitivity to modeling inaccuracies and parameter variations. To mitigate these limitations, hybrid schemes that combine MPC with optimized or intelligent outer-loop controllers have been proposed. For instance, particle swarm optimization (PSO)-tuned PI controllers integrated with MPC have been reported to improve dynamic response and tuning robustness in PV power converters [14]; however, such approaches increase design complexity and remain sensitive to uncertainty in highly non-linear operating conditions.

Recent research trends indicate that cascaded or dual-loop control architectures can effectively exploit the complementary strengths of different control strategies. In such structures, an outer voltage regulation loop ensures robustness and disturbance rejection, while an inner current control loop provides fast dynamic response and accurate tracking. Several dual-loop configurations have been reported in the literature, including conventional PI-PI schemes [15], [16], sliding mode-based outer loops combined with PI current control [17], and learning-based controllers such as deep Q-network-assisted voltage regulation paired with PI current controllers [10]. While these approaches offer improved performance compared to single-loop designs, they often involve trade-offs between robustness, complexity, and computational burden.

Although the above discussion provides a qualitative overview of existing control approaches, a structured synthesis of commonly used strategies is required to clearly position emerging hybrid control architectures. Moreover, a systematic comparative assessment of Type-1 and Type-2 fuzzy logic controllers integrated with model predictive control within a well-defined dual-loop framework remains largely unexplored, particularly under combined irradiance, temperature, and load variations.

Motivated by these observations, this paper proposes a

hybrid dual-loop control strategy for a standalone PV system interfaced with a DC-DC boost converter. The proposed architecture employs a Type-2 fuzzy logic controller in the outer voltage regulation loop to generate a robust reference current, while a model predictive controller is implemented in the inner loop to ensure fast and precise inductor current control. A comparative study is conducted between MPC based on fuzzy logic Type-1 and MPC based on fuzzy logic Type-2 using systematic performance metrics to quantitatively evaluate dynamic response, tracking accuracy, and robustness. In addition, the obtained results are discussed in relation to representative control strategies reported in the recent literature.

The main contributions of this work are summarized as follows.

- Development of a well-defined dual-loop control architecture combining Type-2 fuzzy logic-based voltage regulation with predictive current control model for PV DC-DC boost converters.
- Quantitative comparison between MPC-integrated Type-1 and Type-2 fuzzy logic controllers using systematic dynamic performance indices.
- Comprehensive simulation-based validation under dynamic irradiance, temperature, and load variations, demonstrating improved transient performance and robust disturbance rejection.

The remainder of this paper is organized as follows. Section II presents an overview of the related work. Section III presents the mathematical modeling of the PV array and the DC-DC boost converter. Section IV describes the proposed dual-loop control architecture. Sections V and VI detail the design of the Type-2 fuzzy logic controller and the model predictive current controller, respectively. Section VII discusses the simulation results and comparative performance analysis. Finally, Section VIII concludes the paper and outlines future research directions.

## II. SUMMARY OF RELATED WORK

Although the introduction presented a critical overview of control strategies for photovoltaic DC-DC boost converters, this section provides a concise synthesis of the most representative approaches reported in the literature. The objective is to summarize commonly adopted control techniques and to highlight their typical application domains, strengths, and limitations.

To this end, Table I presents a qualitative comparison of classical, intelligent, and hybrid control strategies used for PV DC-DC boost converters. This summary establishes a consistent reference framework for positioning the advanced dual-loop fuzzy predictive control architecture developed in the subsequent sections.

TABLE I. QUALITATIVE COMPARISON OF CONTROL STRATEGIES FOR PV DC-DC BOOST CONVERTERS.

Control strategy	Efficiency	Applications	Advantages	Limitations
PI [10]	Moderate	Industrial PV systems, low-cost applications	Simple structure, easy implementation, low computational burden	High sensitivity to parameter variations and disturbances, limited robustness
DQN [10]	High	Intelligent and learning-based PV systems	Adaptive behavior, learning capability	High computational burden, training complexity, sensitivity to data quality

Control strategy	Efficiency	Applications	Advantages	Limitations
Type-1 Fuzzy [10]	High	PV converters, non-linear systems	Model-free design, improved robustness over PI	Limited uncertainty handling, performance degradation under strong disturbances
PI + PI [15]	Moderate	Cascaded voltage-current control in PV converters	Simple dual-loop structure, improved stability	Limited adaptability, moderate disturbance rejection
DQN + PI [10]	High	Hybrid intelligent control for PV systems	Fast dynamic response, improved robustness	Increased complexity, dependence on learning process
SMC + PI [17]	High	Robust control of power converters	Strong disturbance rejection, robustness	Chattering phenomenon, increased switching stress
PSO-PI + MPC [14]	High	Optimized predictive control of PV converters	Improved tuning, fast response	Optimization dependency, sensitive to highly non-linear operating conditions

As summarized in Table I, classical linear controllers remain attractive due to their simplicity and low computational cost, but their performance degrades under non-linear and uncertain operating conditions. Intelligent and hybrid control strategies improve adaptability and dynamic response; however, they often introduce increased design complexity, computational burden, or sensitivity to uncertainty.

These examinations highlight the need for advanced dual-loop control architectures capable of combining fast transient response, robust disturbance rejection, and effective uncertainty handling within a unified framework. In this context, the integration of fuzzy logic-based voltage regulation with model predictive current control represents a promising solution, which is investigated in detail in the following sections.

### III. PV ARRAY MODEL

A photovoltaic (PV) array is formed by arranging solar cells in series and parallel configurations. The PV solar cell, fundamentally a p-n junction semiconductor, can be represented using the single-diode model as shown in Fig. 1, which remains the most widely used approach for modeling solar cells.

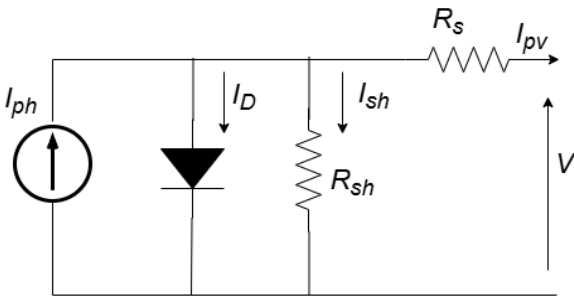


Fig. 1. PV model.

The current-voltage relationship of a photovoltaic cell is delineated by the subsequent equation [18]

$$I_{pv} = I_{ph} - I_s (\exp[(V + IR) / (aV_t n)] - 1) - ((V + IR) / R_{sh}). \quad (1)$$

The current-voltage characteristic of a photovoltaic panel consisting of  $N_s$  cells arranged in series and  $N_p$  cells arranged in parallel is articulated as follows [19]

$$I_{pv} = N_p I_{ph} - N_p I_s (\exp[(q / KT)(V_{pv} / N_s) + (R_s I_{pv} / N_p)] - 1) - (N_p / R_{sh})(V_{pv} / N_s) + (R_s I_{pv} / N_p), \quad (2)$$

where  $I_{pv}$ ,  $I_{ph}$ , and  $I_s$  are the current array, the photo generated, and the reverse saturation current, respectively,  $V$ ,  $V_t$  are the array voltage and the thermal, respectively,  $a$  is the diode ideality factor for the single diode model,  $R_s$ ,  $R_{sh}$  are cell series and shunt resistance,  $N_s$ ,  $N_p$  are the number of modules in series and parallel,  $q$  is the electron charge [ $1.60217646 \times 10^{-19}$  C],  $K$  is the Boltzmann constant [ $1.3806503 \times 10^{-23}$  J/K],  $T$  is the cell temperature, and  $G$  is the irradiance in  $W/m^2$ .

### IV. BOOST CONVERTER MODEL

In this study, only the conventional DC-DC boost converter topology commonly used in standalone photovoltaic systems is considered. The DC/DC boost converter comprises four fundamental external components: an inductor, an electrical switch, a diode, and an output capacitor. It operates in two distinct modes, which are determined by its energy storage capacity and the duration of the switching interval. This converter is commonly employed in photovoltaic (PV) systems to boost output voltage, as illustrated in Fig. 2 [20].

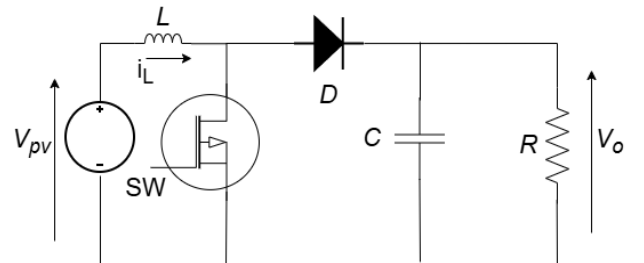


Fig. 2. Boost converter model.

Mode 1: starts when the IGBT is turned on. During this period, the DC voltage source  $V_{pv}$  supplies energy that is stored in the inductor  $L$ , while the capacitor  $C$  discharges through the load resistance  $R$ . The differential equations governing this mode are expressed as follows [19]

$$\begin{cases} \frac{di_L}{dt} = \frac{V_{pv}}{L}, \\ \frac{dV_o}{dt} = \frac{-V_o}{RC}. \end{cases} \quad (3)$$

Mode 2: starts when the IGBT is turned off. In this mode, the energy stored in the inductor is transmitted to the load. The differential equations describing this mode are presented as follows

$$\begin{cases} \frac{di_L}{dt} = \frac{V_{pv}}{L} - \frac{V_o}{L}, \\ \frac{dV_o}{dt} = \frac{i_L}{C} - \frac{V_o}{RC}. \end{cases} \quad (4)$$

The state-space representation of the boost converter can be formulated as follows

$$\begin{cases} \dot{x} = \begin{bmatrix} 0 & \frac{u-1}{L} \\ \frac{1-u}{C} & -\frac{1}{RC} \end{bmatrix} x, \\ y = [0 \quad 1] x, \end{cases} \quad (5)$$

where

$$x = \begin{bmatrix} i_L \\ V_o \end{bmatrix}. \quad (6)$$

## V. PREDICTIVE CURRENT CONTROL

Model predictive control (MPC) is a widely used control approach due to its intuitive design and straightforward implementation. To achieve control goals over a finite prediction horizon, an objective function must be defined. At each sampling point, the optimal solution is determined by selecting a set of control inputs that minimises the objective function while adhering to the discrete-time model of the converter constraints, with the aim of achieving the desired system performance. The primary control input from this sequence is then applied to the process. During the subsequent phase, new state estimates are collected, the prediction horizon advances by one sampling period, and the optimisation procedure repeats [21].

In the predictive current control algorithm, the inductor current is forecast for the subsequent sampling time for all potential switching states of the converter. The switching state that yields the minimum cost function is chosen and activated at the next sampling time. The current prediction is calculated using the Euler discretization formula, as follows [22]

$$x_1(k+1) = x_1(k) + \frac{T_s}{L} V_{pv}(k) - \frac{(1-s)T_s}{L} x_2(k), \quad (7)$$

where  $X_1$  is the current inductor,  $X_2$  is the output voltage of the boost converter, and  $V_{pv}$  is the input voltage.

The final step entails assessing the cost function and determining the optimal control action. This cost function can include the relevant control variables. In the predictive current control method, the primary goal is to regulate the inductor current. Thus, the cost function evaluates the discrepancies between the predicted current values and the reference current. At each sampling instant, the switching state is selected that minimizes this cost function. The cost function is formulated as follows

$$g_{s=0,1} = |x_{1,s=0,1} - x_1^*|, \quad (8)$$

where the current reference  $X_1^*$  is the generated by a Fuzzy

Logic controller.

The implementation of the predictive current control is detailed in Fig. 3.

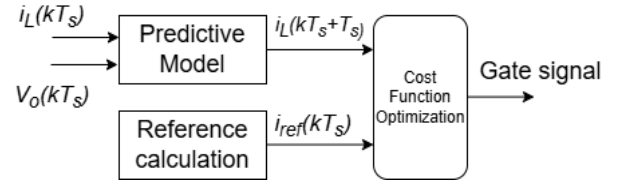


Fig. 3. Predictive model.

## VI. FUZZY TYPE-2 LOGIC CONTROLLER

The Type-2 fuzzy logic controller (T2FLC) extends the traditional Type-1 fuzzy logic controller (T1FLC) by enhancing its ability to handle higher levels of uncertainty. Unlike the Type-1 fuzzy set (T1FS), which uses deterministic membership functions, a Type-2 fuzzy set (T2FS) incorporates uncertainty within its membership functions, allowing for more robust modeling of complex systems. A T2FLC is built in a similar way to a T1FLC, with the key difference being the replacement of the defuzzification stage with an output processing unit. This unit consists of a type reducer, which converts the T2FS into a T1FS, followed by a defuzzifier to produce a crisp output. The ability of T2FLC to handle greater uncertainty makes it especially well suited for applications such as boost converters in photovoltaic systems, where variable conditions such as fluctuating solar input or load changes are common.

Figure 4 illustrates the Type-2 fuzzy membership function. For a specific input value  $X_0$ , the T2FS provides two membership values:  $u_1$ , derived from the upper membership function (UMF), and  $u_2$ , obtained from the lower membership function (LMF). These functions define the bounds of the footprint of uncertainty (FOU), which represents the uncertainty in the membership degree, distinguishing Type-2 fuzzy logic (T2FL) from Type-1. The UMF and LMF enable the T2FLC to model and manage higher levels of uncertainty.

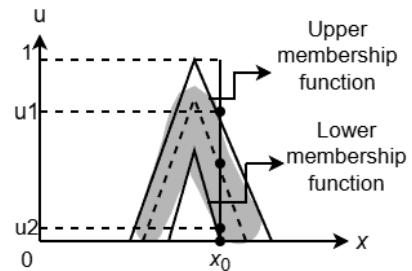


Fig. 4. Type-2 fuzzy membership function.

An interval T2FS, denoted as  $\tilde{A}$ , is characterized by an interval Type-2 membership function  $\mu_{\tilde{A}}(x, u)$ , where  $x \in X$  and  $u \in J_x [0, 1]$  [23]

$$\tilde{A} = \left\{ ((x, u), \mu_{\tilde{A}}(x, u)) \mid \forall x \in X, \forall u \in J_x \subseteq [0, 1] \right\}, \quad (9)$$

in which  $0 \leq \mu_{\tilde{A}}(x, u) \leq 1$ .  $\tilde{A}$  can also be expressed as

$$\tilde{A} = \int_{x \in X} \int_{u \in J_x} \mu_{\tilde{A}}(x, u) / (x, u) J_x \subseteq [0, 1]. \quad (10)$$

The  $(\int)$  in (10) represents all acceptable  $x$  and  $u$  spaces.

With  $\forall u \in J_x [0, 1]$ ,  $J_x$  is the fundamental membership function of  $x$ . Moreover, each primary and secondary membership has equivalent values.

The core membership functions of the T2FS are uncertain. The T2FS consists of a restricted region. This region is named the FOU. Mathematically, the FOU is a combination of all primary membership functions (MFs)

As illustrated in Fig. 5, the MF of a generic T2FS is three-dimensional. The MF of the set is established using the border of the cross-section alone.

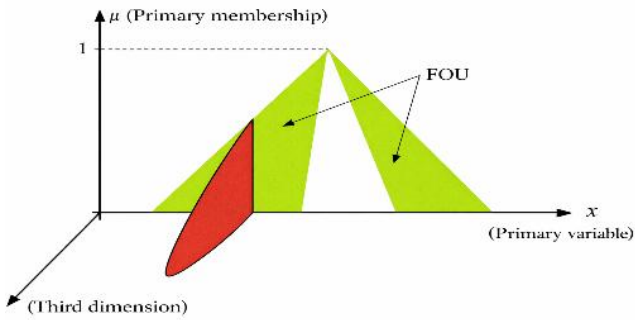


Fig. 5. Type-2 fuzzy membership function.

In a Type-2 fuzzy logic system, each rule produces an output set that is itself a T2FS. The type reducer then aggregates these Type-2 output sets, similar to how a Type-1 defuzzifier combines T1FSs in a Type-1 fuzzy logic (T1FL) system, as described by Mendel in his work on Type-2 fuzzy systems and type reduction [24]. Following this, a centroid calculation is performed on the aggregated T2FS, resulting in a reduced set, which is T1FS. This T1FS can then be defuzzified to obtain a crisp output for practical use. The type reduction step is crucial in T2FS as it bridges the gap between the complex uncertainty modeling of Type-2 sets and the simpler, actionable output needed for control applications, such as regulating a boost converter's voltage in photovoltaic systems. Common-type reduction methods include the Karnik-Mendel algorithm, which iteratively computes the centroid by considering the bounds of the FOU.

In alignment with the T1FL controller, the T2FSs are designated with labels including Negative (NE), Zero (ZE), and Positive (PO) to define their linguistic variables. The proposed cascaded controller employs a T2FL controller in the outer loop to regulate the voltage to a reference value of 600 V, with an inner loop controlling the inductor current using predictive control. Details are provided in Fig. 6.

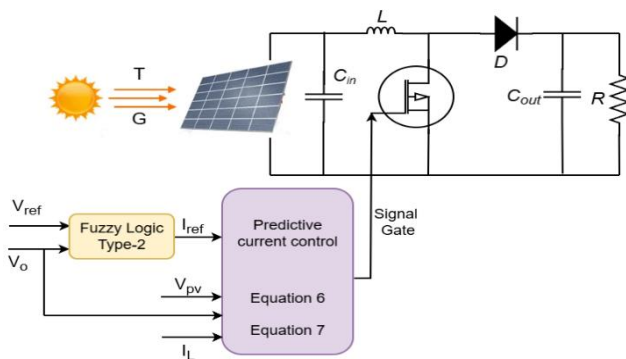


Fig. 6. Proposed controller.

The fuzzy logic controller was developed utilizing a heuristic rule base defined by voltage error and error variation. Input and output membership functions were selected to ensure smooth control action and steady voltage regulation. For the T2FL controller, uncertainty was integrated through the footprint of uncertainty applied to the membership functions, boosting resilience against modeling inaccuracies and external disturbances. Overall, the design technique consisted of identifying the input and output variables, developing appropriate membership functions, formulating the rule base, and applying a defuzzification method to generate the control signal.

## VII. DISCUSSION AND RESULTS

This section presents a comprehensive evaluation of the proposed hybrid dual-loop control strategy based on Type-2 fuzzy logic voltage regulation and model predictive current control. The performance of the proposed approach is simulated by using Matlab/Simulink environment and systematically compared with the Type-1 fuzzy logic predictive control under the same operating conditions. The evaluation is carried out using a simulation framework that includes variations in irradiance, temperature, and load.

All simulations presented in this study are based on theoretical and mathematical models of the photovoltaic array and the DC-DC boost converter. System behavior is evaluated under realistic operating conditions, including irradiance, temperature, and load variations to emulate practical operating conditions.

The simulation was performed with the parameters given in Table II. The fuzzy logic controllers are designed using consistent linguistic variables and rule bases, as illustrated in Figs. 7 and 8 and summarized in Table III. This unified structure ensures a fair comparison between Type-1 and Type-2 fuzzy logic strategies. The dual-loop architecture consists of an outer voltage regulation loop that generates the reference current and an inner predictive current control loop that ensures fast inductor current tracking.

The environmental test conditions, shown in Figs. 9 and 10, introduce realistic and severe operating scenarios, including simultaneous irradiance and temperature variations. Furthermore, a load variation of 4 ohms to 5 ohms was applied at  $t = 5$  seconds. Such conditions allow for an effective evaluation of the robustness and transient performance of the proposed control strategy.

TABLE II. SYSTEM PARAMETERS.

Parameters	Values
Power	100 kW
Input Capacitor	100 $\mu$ F
Output Capacitor	6000 $\mu$ F
Inductor	5 mH
Switching frequency	5 kHz
Open circuit voltage ( $V_{oc}$ )	64.2 V
Short-circuit current ( $I_{sc}$ )	5.96 (A)
Voltage at maximum power point ( $V_{mp}$ )	54.7 V
Current at maximum power point ( $I_{mp}$ )	5.58 A
Shunt resistance $R_{sh}$	393.2054 $\Omega$
Series resistance $R_s$	0.37428 $\Omega$
Series-connected modules per string	5
Parallel strings	66

TABLE III. FUZZY LOGIC SETS.

$\Delta E$ \ E	E	NE	ZE	PO
NE	NE	NE	NE	PO
ZE	NE	NE	ZE	PO
PO	NE	PO	PO	PO

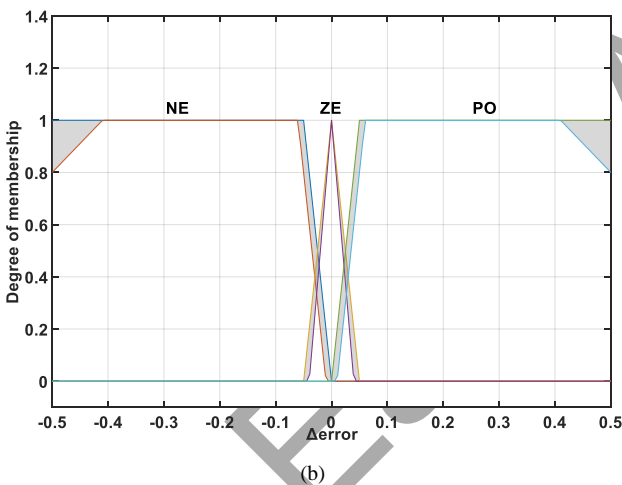
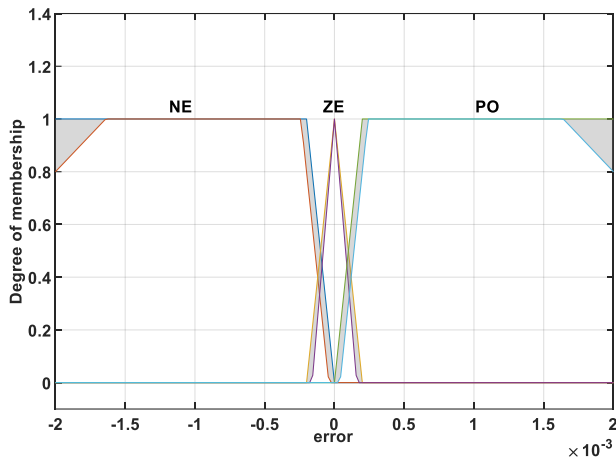
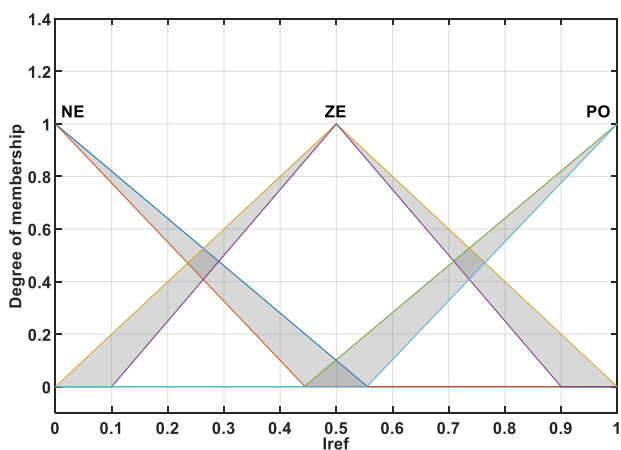
Fig. 7. Inputs membership functions of T2FLC: (a) E; (b)  $\Delta E$ .

Fig. 8. Output membership functions of T2FLC.

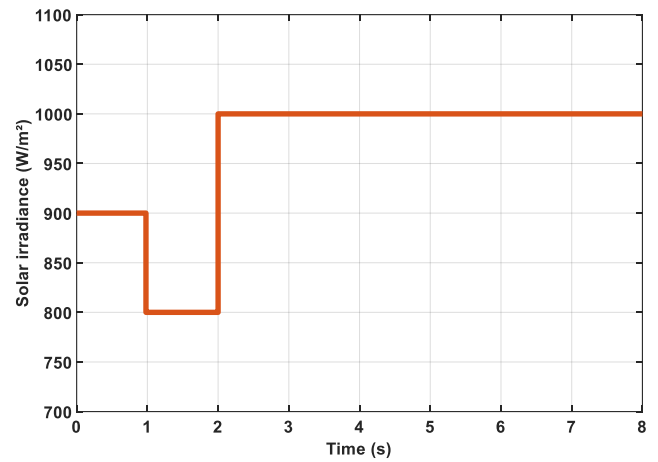


Fig. 9. Solar irradiance variation profile used for performance evaluation.

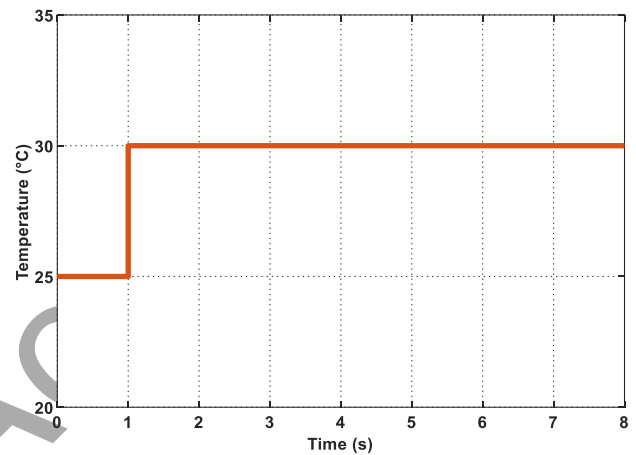


Fig. 10. Ambient temperature variation profile used for performance evaluation.

At this stage, the converter is modeled in the MATLAB/Simulink environment using elements of the SimPowerSystems package, instead of the numerical dynamical equations in (5), to accurately depict its nature. The sampling period chosen for the simulations is  $8 \mu\text{s}$ .

Figure 11 presents the output voltage responses obtained using the Type-1 and Type-2 fuzzy predictive controllers under combined irradiance, temperature, and load variations. The results demonstrate that both controllers successfully regulate the output voltage (600 V) and reject external disturbances without steady-state error. Furthermore, no overshoot was observed for both control strategies, indicating stable and effective transient behavior despite the boost converter's non-minimum phase characteristics. However, as shown in Fig. 12, a quantitative analysis reveals that the Type-2 fuzzy predictive controller achieves a faster dynamic response, where the response and settling times are reduced by approximately 21.05% compared to the Type-1 fuzzy predictive controller. This improvement demonstrates the benefit of incorporating uncertainty modeling into the fuzzy logic framework, as it allows for the generation of a more accurate reference current for the predictive current control loop.

As shown in Fig. 13, the responses of the inductor current further confirm the effectiveness of the proposed control strategy. Accurate and rapid current tracking is achieved in both cases, which validates the suitability of model predictive

control for inner-loop regulation. However, the Type-2 fuzzy logic controller improves current reference generation, resulting in a faster response.

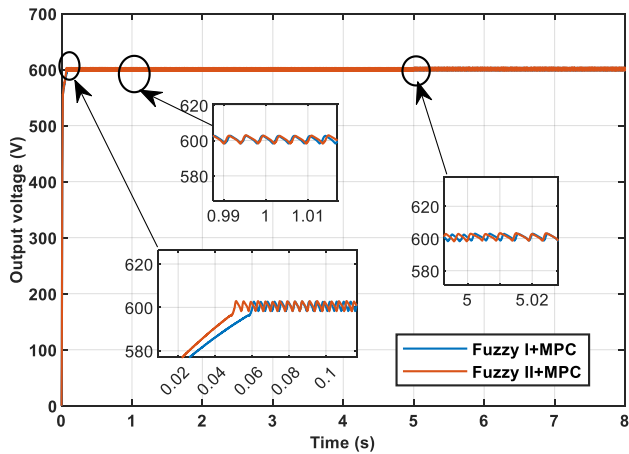


Fig. 11. Comparison of output voltage dynamic response between Type-1 and Type-2 fuzzy predictive controllers under variations in irradiance, temperature, and load.

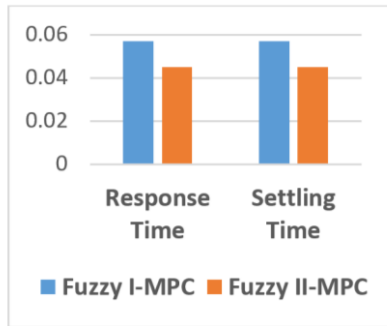


Fig. 12. Comparison of response time and settling time for fuzzy predictive control strategies.

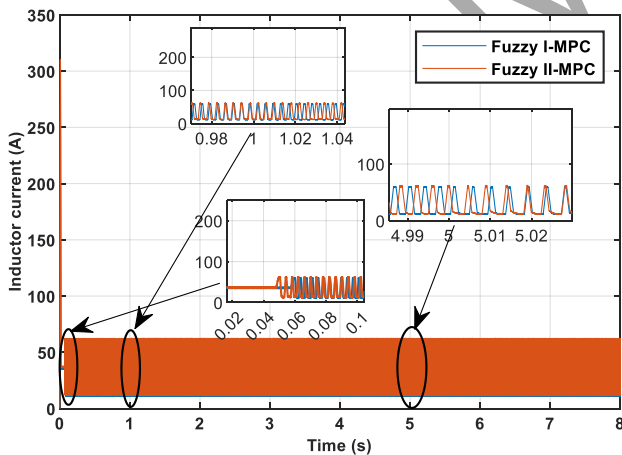


Fig. 13. Inductor current tracking performance under varying environmental conditions.

Further insight is gained through evaluating integral performance indices, such as integral absolute error (IAE), integral squared error (ISE), integral time squared error (ITSE), and integral time absolute error (ITAE), as summarized in Table IV and Fig. 14. The Type-2 fuzzy predictive controller yields consistently lower values across all indices, indicating reduced tracking error and improved dynamic efficiency compared to the Type-1 controller.

TABLE IV. INTEGRAL PERFORMANCE INDICES FOR FUZZY PREDICTIVE CONTROL STRATEGIES.

	IAE	ISE	ITSE	ITAE
Fuzzy I + MPC	7.087	2240	13.31	0.1339
Fuzzy II + MPC	6.904	2235	13.04	0.1261

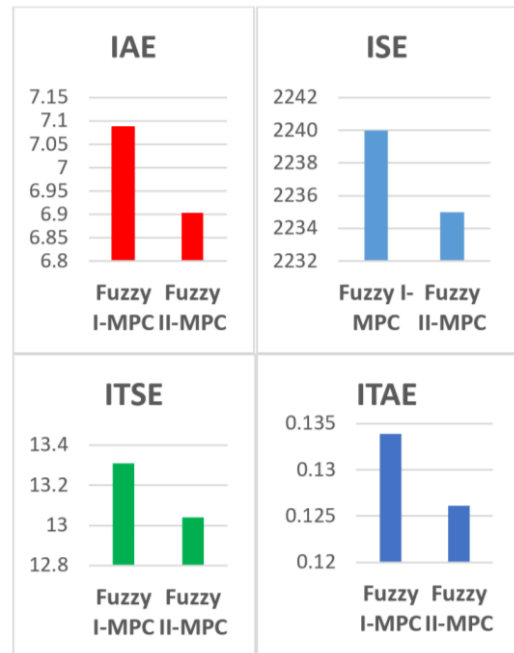


Fig. 14. Comparison of integral performance indices for fuzzy predictive control strategies.

A larger comparison with existing control strategies documented in the literature is summarized in Table V. Classical approaches, such as proportional-integral control, and hybrid methods, including sliding mode and learning-based controllers, often deliver adequate regulation, but often have longer settling times or are more sensitive to perturbations. By comparison, the proposed dual-loop Type-2 fuzzy predictive architecture delivers a quick dynamic response, zero overshoot, and robust disturbance rejection inside a single control framework.

TABLE V. QUANTITATIVE PERFORMANCE COMPARISON OF CONTROL STRATEGIES.

Controller	Response time	Settling Time	Overshoot	Sensitivity to Disturbances
PI [10]	0.06 s	0.14 s	High	High
DQN [10]	0.35 s	0.4 s	Low	Moderate
Fuzzy I [10]	0.05 s	0.04 s	Low	Moderate
PI + PI [15]	0.06 s	0.1 s	Low	Moderate
DQN + PI [10]	0.02 s	0.04 s	Very Low	Low
PSO-PI + MPC [14]	0.05 s	0.06 s	None	Low
SMC + PI [17]	0.05 s	0.1 s	None	Disturbance rejection
Fuzzy I + MPC	0.057 s	0.057 s	None	Disturbance rejection
Fuzzy II + MPC [Proposed]	0.045 s	0.045 s	None	Disturbance rejection

Overall, the results demonstrate that while both fuzzy predictive controllers are capable of ensuring stable voltage regulation and disturbance rejection, the Type-2 fuzzy logic

predictive control strategy offers measurable improvements in response speed, settling behavior, and error tracking. These advantages make the proposed approach particularly suitable for photovoltaic DC-DC boost converter applications operating under highly variable environmental and load conditions.

From a practical standpoint, the provided dual-loop control technique can be applied in real-time digital controllers for solar power converters, as it combines rule-based fuzzy inference with a computationally efficient predictive current control scheme. The improved transient response and disturbance rejection capability lead to enhanced voltage stability and lower stress on power electronic components, which are crucial for standalone photovoltaic applications.

### VIII. CONCLUSIONS

This paper has presented a hybrid dual-loop control strategy for photovoltaic DC-DC boost converters that combines Type-2 fuzzy logic voltage regulation with model predictive current control. The proposed architecture was designed to address the inherent non-linearity, uncertainty, and disturbance sensitivity of photovoltaic energy conversion systems operating under variable environmental and load conditions.

A well-defined simulation framework that incorporates variations in irradiance, temperature, and load was used to evaluate the performance of the proposed approach. The results demonstrated that both Type-1 and Type-2 fuzzy predictive control strategies are capable of ensuring stable voltage regulation, zero overshoot, and effective disturbance rejection. However, a comparative analysis revealed that the Type-2 fuzzy logic predictive controller provides superior dynamic performance, achieving a faster response, with an improvement of approximately 21.04 % compared to the Type-1 fuzzy predictive controller, while maintaining zero overshoot and reduced settling time. The improved performance is attributed to the enhanced uncertainty handling capability of Type-2 fuzzy logic. Furthermore, the evaluation of the integral performance indices confirmed the improved tracking accuracy and dynamic efficiency of the proposed control strategy. The results obtained illustrate the advantages of merging intelligent uncertainty-aware control with model-based predictive approaches inside a cascaded dual-loop framework. This combination offers a balanced approach that ensures fast transient response, robust voltage regulation, and high disturbance rejection for photovoltaic boost converter applications.

Future work will focus on extending the proposed control strategy to experimental validation. Additional investigations may also include the application of the proposed approach to advanced converter topologies and grid-connected photovoltaic systems.

### CONFLICTS OF INTEREST

The authors declare that they have no conflicts of interest.

### REFERENCES

- [1] W. Strielkowski, L. Civiń, E. Tarkhanova, M. Tvaronavičienė, and Y. Petrenko, "Renewable energy in the sustainable development of electrical power sector: A review", *Energies*, vol. 14, no. 24, p. 8240, 2021. DOI: 10.3390/en14248240.
- [2] Md K. G. Deshmukh, M. Sameeroddin, D. Abdul, and M. A. Sattar, "Renewable energy in the 21st century: A review", *Materials Today: Proceedings*, vol. 80, part 3, pp. 1756–1759, 2023. DOI: 10.1016/j.matpr.2021.05.501.
- [3] O. E. Olabode, I. K. Okakwu, D. O. Akinyele, T. O. Ajewole, S. Oyelami, and O. V. Olisa, "Effect of ambient temperature and solar irradiance on photovoltaic modules' performance", *Iranica Journal of Energy and Environment*, vol. 15, no. 4, pp. 402–420, 2024. DOI: 10.5829/ijee.2024.15.04.08.
- [4] A. Durusu, I. Nakir, A. Ajder, R. Ayaz, H. Akca, and M. Tanrioven, "Performance comparison of widely-used maximum power point tracker algorithms under real environmental conditions", *Advances in Electrical and Computer Engineering*, vol. 14, no. 3, pp. 89–94, 2014. DOI: 10.4316/aee.2014.03011.
- [5] A. A. Bakar, W. M. Utomo, T. Taufik, S. Aizam, and Jumadri, "DC/DC boost converter with PI controller using real-time interface", *ARN Journal of Engineering and Applied Sciences*, vol. 10, no. 19, pp. 9078–9082, 2015.
- [6] S. Pandey, B. Dwivedi, and A. Tripathi, "Performance analysis of SMC controlled PV fed boost converter", in *Proc. of 2016 7th India International Conference on Power Electronics (IICPE)*, 2016, pp. 1–4. DOI: 10.1109/IICPE.2016.8079544.
- [7] T. L. Rao, N. T. Rao, G. Ashok, and M. M. Sankar, "DC/DC boost converter using adaptive fuzzy logic controller", *IOP Conference Series: Earth and Environmental Science*, vol. 1529, art. 012031, 2025. DOI: 10.1088/1755-1315/1529/1/012031.
- [8] H. G. Eleraky, A. Refaat, A. Kalas, and A. F. Abouzeid, "Performance assessment of artificial neural networks-based MPPT technique for photovoltaic systems", in *Proc. of 2024 14th International Conference on Electrical Engineering (ICEENG)*, 2024, pp. 48–53. DOI: 10.1109/ICEENG58856.2024.10566372.
- [9] R. I. Areola, O. A. Aluko, and O. I. Dare-Adeniran, "Modelling of adaptive neuro-fuzzy inference system (ANFIS)-based maximum power point tracking (MPPT) controller for a solar photovoltaic system", *Journal of Engineering Research and Reports*, vol. 25, no. 9, pp. 57–69, 2023.
- [10] P. Nie, Y. Wu, Z. Wang, S. Xu, S. Hashimoto, and T. Kawaguchi, "The voltage regulation of boost converters via a hybrid DQN-PI control strategy under large-signal disturbances", *Processes*, vol. 13, no. 7, p. 2229, 2025. DOI: 10.3390/pr13072229.
- [11] N. N. Karnik, J. M. Mendel, and Qilian Liang, "Type-2 fuzzy logic systems", *IEEE Transactions on Fuzzy Systems*, vol. 7, no. 6, pp. 643–658, 1999. DOI: 10.1109/91.811231.
- [12] O. F. Bay and M. O. Yatak, "Type-2 fuzzy logic control of a photovoltaic sourced two stages converter", *Journal of Intelligent & Fuzzy Systems: Applications in Engineering and Technology*, vol. 35, no. 1, pp. 1103–1117, 2018. DOI: 10.3233/JIFS-17865.
- [13] M. Ahmed, I. Harbi, R. Kennel, J. Rodríguez, and M. Abdelrahem, "Maximum power point tracking-based model predictive control for photovoltaic systems: Investigation and new perspective", *Sensors*, vol. 22, no. 8, p. 3069, 2022. DOI: 10.3390/s22083069.
- [14] N. Cherigui, A. Chemidi, and A. Tahour, "Dual-loop control strategy for a standalone PV boost converter using PSO-tuned PI and model predictive current control", in *Proc. of 9th International Conference on Artificial Intelligence in Renewable Electronic Systems*, 2025.
- [15] T.-L. Le, L. V. Truc, and T. N. Tien, "Cascaded PI-controlled multistage boost converter for low-voltage renewable sources", *Engineering, Technology & Applied Science Research*, vol. 15, no. 5, pp. 26777–26782, 2025. DOI: 10.48084/etasr.12941.
- [16] O. Rabiaa, B. H. Mouna, S. Lassaad, F. Aymen, and A. Aicha, "Cascade control loop of DC-DC boost converter using PI controller", in *Proc. of 2018 International Symposium on Advanced Electrical and Communication Technologies (ISAECT)*, 2018, pp. 1–5. DOI: 10.1109/ISAECT.2018.8618859.
- [17] B. Torchani *et al.*, "Adaptive sliding mode control based on maximum power point tracking for boost converter of photovoltaic system under reference voltage optimizer", *Frontiers in Energy Research*, vol. 12, ID 1485470, 2024. DOI: 10.3389/fenrg.2024.1485470.
- [18] R. S. Pranasundaram and G. Chandrasekaran, "Innovative Narwhal MPPT with feed forward decoupling for enhanced solar grid integration", *Elektronika ir Elektrotechnika*, vol. 31, no. 4, pp. 52–61, 2025. DOI: 10.5755/j02.eie.42909.
- [19] N. J. Mlazi, M. Mayengo, G. Lyakurwa, and B. Kichonge, "Mathematical modeling and extraction of parameters of solar photovoltaic module based on modified Newton–Raphson method", *Results in Physics*, vol. 57, art. 107364, 2024. DOI: 10.1016/j.rinp.2024.107364.
- [20] N. Cherigui, A. Chemidi, A. Tahour, and M. Horch, "A new advanced third-order sliding mode control with adaptive gain adjustment using fuzzy logic technique for standalone photovoltaic systems", *AIMS*

*Electronics and Electrical Engineering*, vol. 9, no. 2, pp. 243–259, 2025. DOI: 10.3934/electreng.2025012.

- [21] H.-J. Ko, H.-G. Koh, and Y.-J. Choi, “A model predictive current control method for achieving a high efficiency and high robustness boost PFC converter operation”, *IEEE Access*, vol. 11, pp. 142754–142763, 2023. DOI: 10.1109/ACCESS.2023.3343124.
- [22] Y. Li, T. Dragičević, S. Sahoo, Y. Zhang, and F. Blaabjerg, “An improved model predictive control for DC-DC boost converter”, in *Proc. of 2022 IEEE 13th International Symposium on Power*
- Electronics for Distributed Generation Systems (PEDG)*, 2022, pp. 1–6. DOI: 10.1109/PEDG54999.2022.9923104.
- [23] I. Atacak and O. F. Bay, “A type-2 fuzzy logic controller design for buck and boost DC–DC converters”, *Journal of Intelligent Manufacturing*, vol. 23, no. 4, pp. 1023–1034, 2012. DOI: 10.1007/s10845-010-0388-1.
- [24] J. M. Mendel and R. I. B. John, “Type-2 fuzzy sets made simple”, *IEEE Transactions on Fuzzy Systems*, vol. 10, no. 2, pp. 117–127, 2002. DOI: 10.1109/91.995115.



This article is an open access article distributed under the terms and conditions of the Creative Commons Attribution 4.0 (CC BY 4.0) license (<http://creativecommons.org/licenses/by/4.0/>).

Early Access